

Anomalous deep-level transients related to quantum well piezoelectric fields in $\text{In}_y\text{Ga}_{1-y}\text{N}/\text{GaN}$ -heterostructure light-emitting diodes

L. Rigutti,* A. Castaldini, and A. Cavallini

Physics Department, University of Bologna, Viale Bertoni 6/2, 40127 Bologna, Italy

(Received 31 August 2007; published 11 January 2008)

The anomalous inversion of capacitance transients was observed during deep level transient spectroscopy characterization of InGaN/GaN based blue light-emitting diodes. Deep level C ($E_C - E_T = 0.25$ eV), a majority carrier trap related to isolated point defects, has a negative transient when the bias stimulates it only in the bulk region and has a positive transient when the filling pulse is such that the quantum well (QW) region is probed. We explain this observation by a model based on the confining effects of QW piezoelectric fields on the charge emitted by deep levels. Instead of being collected by the junction, this charge is rearranged in conduction band states of the multi-QW region, shifting its center of mass toward the bulk. We measured the strength of piezoelectric fields (2.3 MV/cm) and the QW In fraction ($x=0.15$) by means of photocurrent spectroscopy, and we tested the accuracy of our model by comparing a Schrödinger-Poisson simulation with our experimental data, finding substantial agreement.

DOI: [10.1103/PhysRevB.77.045312](https://doi.org/10.1103/PhysRevB.77.045312)

PACS number(s): 73.40.Kp, 73.20.Hb, 73.21.Fg, 78.30.Fs

I. INTRODUCTION

The polarization properties of nitride materials have been the object of a wide number of studies in the past decade.¹⁻⁷ Especially in multiquantum well (MQW) systems, widely used in optoelectronic devices such as lasers, light-emitting diodes (LEDs), and modulators, spontaneous and piezoelectric polarizations, arising at the heterostructure interfaces have important consequences on a wide class of optoelectronic and electrical properties of the device. The quantum-confined Stark effect in InGaN/GaN/AlGaIn quantum wells (QWs), for instance, is basically different from those in analogous systems based on nonpolar materials.⁴⁻⁸ Moreover, it has been shown that the strong modifications to the band profiles in the junction region have important effects on the current transport,⁹ as well as the capacitance-voltage (C - V) characteristics^{10,11} of nitride-based p - n heterojunctions and MQW systems.

Deep level transient spectroscopy (DLTS) in semiconductor heterostructures, mostly transistor [high electron mobility transistor and heterostructure field effect transistor (HFET)] and optoelectronic structures (LEDs and lasers), is a widely used technique for the characterization of interfacial and surface defect states, as well as bulk defect states.¹²⁻¹⁴ In some cases, by means of this technique, it is also possible to characterize conduction band states inside the quantum wells,¹⁵⁻¹⁸ although care must be taken in order not to confuse emission from deep levels localized in the QW region with emission from QW conduction or valence band states.¹⁹ Heterostructures also give rise to observations related to deep level transients which do not occur when characterizing homogeneous materials and junctions. Among these, the inversion of current transients in current-DLTS performed in HFET structures¹² and the appearance of positive capacitance transients (usually related to minority carrier emission) in reversely biased p - n junctions with a filling pulse level still having negative values, i.e., not able to produce an injection of minority carriers in the analyzed region, have been studied.²⁰ In all these cases, it is essential to know which part of the structure is probed during the experiment, i.e., which

portion of the structure contains the deep levels, the occupation of which is changed during the bias pulse. This knowledge can be reached with a satisfying degree of accuracy by complementary experimental techniques, such as capacitance-voltage (C - V) profiling, photocurrent (PC) spectroscopy, and other electrical and optical characterization techniques, as well as by computer simulation of the electro-optical properties of the structure.

In this work, we characterize LED test structures by means of DLTS, finding that the capacitance transients related to majority carrier emission invert depending on the bias parameters used. Comparing the DLTS bias parameters with the apparent charge profile from C - V characterization, we find that the inversion occurs when the DLTS filling pulse probes the QW region, and the reverse bias is such that the QW region is depleted. We relate this set of observations to the existence of piezoelectric fields in the MQW system. The inversion of the capacitance transient is thus an effect of polarization fields, the strength of which is estimated by means of PC spectroscopy. This inversion is due to the suppressed collection of carriers emitted from deep levels because of the presence of an average positive field in the MQW system opposite to the negative junction field. This means that the charge emitted from deep levels can still be trapped in conduction band states in the MQW system when the reverse bias is restored, with consequent negative effects for device operation at high frequencies. This conduction band charge may also give rise to a nonradiative recombination when the junction is switched to positive bias, thus lowering the quantum efficiency and frequency response.

The work is organized as follows. Section II describes the experimental details regarding analyzed samples and instrumentation. Section III exposes the results. By means of photocurrent spectroscopy (Sec. III A), we determine the strength of the piezoelectric field in the active quantum wells, finding that it is high enough to provide an average field more intense than and opposite to the junction field. Capacitance-voltage (C - V) characterization is presented in Sec. III B; from these results, we obtain the information for adequately probing the different regions of the junction by

means of DLTS. The results of this technique are shown in Sec. III C. We show here how the dominant peak inverts depending on the bias parameters used. In Sec. III D, we investigate more thoroughly the nature of the dominant deep level, excluding that it is associated with extended defects having potential barrier. In Sec. IV, we discuss the results and formulate the hypothesis on which the explanation of the transient inversion is based: this is due to the opposition of the piezoelectric field to the junction field, which prevents the charge emitted after the forward bias pulse from being collected by the junction. This charge is rearranged, after emission from deep traps, to conduction band states in the whole QW region, shifting its center of mass deeper toward the bulk but remaining in the MQW system. We show how this can yield a positive capacitance transient (Sec. IV A). In Sec. IV B, we simulate the conduction band charge distributions in a typical junction structure, showing that the forward bias pulse injects electrons almost only in the first QW (closest to the junction), and that electrons emitted from deep traps after the pulse cannot be collected by the junction field, being rearranged in the MQW region with their center of mass deeper toward the bulk. In Sec. IV C, we finally compare the predictions of model and simulation with our experimental results, showing that they are in substantial agreement.

II. EXPERIMENTAL DETAILS

The vertical structure of the device consists of an n -doped SiC substrate, a low-temperature buffer layer, a 2 μm thick Si-doped GaN layer (nominal doping concentration $N_D=5 \times 10^{17} \text{ cm}^{-3}$), an active region with a fourfold InGaN/GaN multiple quantum well system, a 100 nm thick heavily Mg-doped AlGaIn cladding layer, and a 200 nm heavily Mg-doped GaN contact layer. The structure was grown along the crystallographic c axis, so that polarization fields parallel to the basal plane arise at the abrupt interfaces between layers with different alloy compositions. Squared chips with 250 μm sides, bonded on metallic packages TO18 with a bicomponent epoxy resin acting as Ohmic cathode contact, have been studied.

Photocurrent spectra were collected at room temperature; light from a QTH lamp with enhanced UV emission was chopped at $f=16$ Hz, monochromatized in a CornerStone 260 monochromator with spectral resolution $\Delta\lambda=1$ nm, and directed on to the sample. The photocurrent signal was collected by a SR 830 lock-in amplifier. External quantum efficiency (EQE) spectra were calculated, dividing the photocurrent spectra by the spectral photon flux previously measured by means of a thermopile detector with flat response in the analyzed spectral region.

C - V measurements were performed at room temperature and at $T=217$ K at 1 MHz frequency with a Boonton 7200 capacitance meter, and the apparent charge profiles as a function of depth $n_{CV}(x)$ and as a function of reverse bias $n_{CV}(V_b)$ were calculated by approximating the junction as p^+n . I - V characteristics were collected by means of a Keithley 6517 electrometer, with sensitivity in the range of tens of picoamperes.

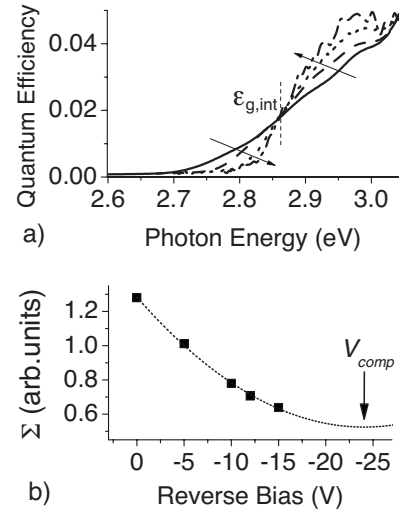


FIG. 1. (a) Quantum well edge of the photocurrent spectra evidencing the blueshift of the absorption edge with increasing reverse bias, as indicated by the arrows. Spectra were collected with $V_b = 0$ V (solid line), $V_b = -5$ V (dashed line), $V_b = -10$ V (dotted line), and $V_b = -15$ V (dash-dotted line). (b) The quantity Σ defined in Eq. (1) as a function of the reverse bias and the second order polynomial fitting the data. The minimum of the parabola indicates the value of the compensation voltage V_{comp} .

DLTS measurements have been performed in the temperature interval of 100–300 K; the spectra were collected with different values of reverse bias V_b and filling pulse V_{fill} , in order to probe different regions of the n side of the junction, and with different values of filling pulse duration t_p , in order to investigate the capture kinetics of the dominant level. The capacitance transients were analyzed by means of a SULA Technologies deep level spectrometer with exponential correlator.

III. RESULTS

A. Determination of piezoelectric field strength

The experimental determination of the strength of the piezoelectric fields arising in the InGaN/GaN quantum well embedded in a light-emitting diode is possible with several experimental techniques, including photoluminescence,^{2,5} electroabsorption,⁶ and PC.^{4,7} This latter technique is very accurate, provided the sample under study allows the observation of the so-called compensation voltage, in conditions usually satisfied in purposely designed p - i - n junctions.⁴ In this work, we found the piezoelectric field by means of photocurrent, in a slight variation of the technique described by Fransen *et al.*⁷ This technique is based on the measurement of the external bias V_{comp} compensating the piezoelectric field in the quantum well. This compensation is analyzed by observing the bias-dependent shift of the absorption edge in the EQE spectra obtained by normalization of the PC spectra by the photon flux.

In Fig. 1, we report the EQE spectra of the analyzed sample in the region of the absorption edge of the QW, collected at different applied bias. It is possible to observe the

blueshift of the absorption edge induced by the increasing reverse bias, as well as the intersection of all curves at the same energy point $\varepsilon_{g,int}=2.86$ eV, a peculiarity already reported in the photocurrent study of blueshift in $\text{In}_{0.08}\text{Ga}_{0.92}\text{N}/\text{GaN}$ QWs.⁷ This value is assumed to be the actual gap of the QW. A slight modulation is superimposed on the spectra due to the occurrence of interference effects in the multilayer structure. The compensation voltage is the applied bias minimizing the following integral:⁷

$$\Sigma(V_b) = \int_0^{\varepsilon_{g,int}} S(\varepsilon, V_b) d\varepsilon, \quad (1)$$

where $S(\varepsilon, V_b)$ is the EQE signal at photon energy ε and bias V_b . In the present case, we found this minimum by extrapolation, performed with a second-order polynomial fit of the values of Σ (see inset of Fig. 1). The value of the compensation voltage is $V_{comp} = -24 \pm 1$ V. A more accurate determination of the value of V_{comp} could not be achieved due to the structural parameters of the junction: in fact, photocurrent signal at $|V_b| > 15$ V was too noisy to allow the collection of the spectra.

From V_{comp} , it is then possible to calculate the piezoelectric field by knowing the structural parameters through the formula⁷

$$F_{pz} = -\frac{q}{\varepsilon_s} \frac{N_A N_D}{N_A + N_D} d_{bar} + \frac{q}{\varepsilon_s} \sqrt{\frac{N_A^2 N_D^2}{(N_A + N_D)^2} d_{bar}^2 + \frac{2\varepsilon_s (V_{bi} + V_{comp})}{q} \frac{N_A N_D}{N_A + N_D}}, \quad (2)$$

with N_A and N_D the acceptor and donor concentrations in the p - and n -type layers, respectively, ε_s the semiconductor dielectric constant, q the elementary charge, V_{bi} the built-in voltage, and d_{bar} the sum of all barrier widths. This formula requires the knowledge of the structural parameter d_{bar} and is valid only for abrupt junctions with uniform doping density.

Another procedure for the determination of the piezoelectric field at the compensation voltage is the comparison with the maximum junction field of a biased p - n junction,²¹

$$F_{pz} \cong -F_{max}(V_{comp}) = \frac{2(V_{bi} - V_{comp})}{w(V_{comp})} = \frac{2(V_{bi} - V_{comp})}{\varepsilon_s} C(V_{comp}), \quad (3)$$

where $w(V_b)$ is the depletion region width and $C(V_b)$ is the capacitance per unit area at the applied bias V_b . This calculation is independent of structural parameters, which implicitly determine the dependence of the experimentally measured C on V_b . The maximum junction field approximates the one actually superimposed to the piezoelectric field, because the MQW region is not exactly located at the junction point. However, C - V characterization indicates that the MQW region is much closer to the junction point than to the depletion region edge at V_{comp} , so that the approximation given by Eq. (2) is valid.

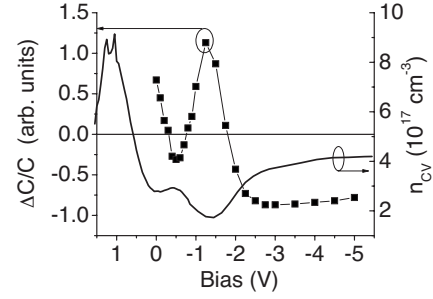


FIG. 2. Apparent carrier profile (solid line, referred to right Y axis) and the peak DLTS signal at $e_n=46.5$ s⁻¹ (squares, referred to left Y axis) at $T=217$ K from a multi-QW LED. The DLTS signal was measured with filling pulse V_{fill} and reverse bias V_b (the latter appearing as abscissa coordinate) related by $V_{fill}=V_b+1$ V.

For the determination of the piezoelectric field, the result from Eq. (2), assuming $N_A \gg N_D = 4 \times 10^{17}$ cm⁻³ (the bulk concentration measured by C - V profiling) and $d_{bar}=30$ nm, yields $F_{pz}=2.31 \pm 0.05$ MV/cm, while calculation from Eq. (3), considering the value of the capacitance at V_{comp} , yields $F_{pz}=2.3 \pm 0.1$ MV/cm, in excellent agreement with the previous value.

The value of $\varepsilon_{g,int}=2.86$ eV corresponds, according to the results of Wu *et al.*,²² to an In fraction $x=0.15$. The theoretical value of the QW piezoelectric field predicted for this In fraction³ is $F_{pz}=2.65$ MV/cm, in good agreement with our estimate.

The value found for the piezoelectric field in our QW region is sufficiently intense for a strong modification of the band profile in the junction region of the device. Thus, there is a positive net average field in the MQW region, opposed to the negative junction field. The effects of this net average field on the charge distribution during voltage pulses occurring during DLTS will be discussed in Sec. III.

B. Capacitance-voltage charge profiling

Capacitance-voltage profiling of MQW junctions is an extremely sensitive technique for the investigation of structural properties. The charge profile n_{CV} and the junction depth x obtained by the standard calculation²¹ can be shown to reproduce the actual depth of the quantum well system and the doping concentration in the bulk of the junction.^{23,24} If the QWs are sufficiently spaced, C - V profiling makes it also possible to determine the number of QWs in the junction; structures for device applications such as those under investigation do not allow the resolution of the number of QWs.

In Fig. 2, the apparent charge profile versus applied bias $n_{CV}(V_b)$ is reported. When $1.5 > V_b > -1$ V, the edge of the space charge layer crosses the MQW region. Rigorously speaking, one could not even define an edge of the space charge region because in this bias interval, there is no net separation between one spatial region depleted of conduction band carriers, and another with conduction band carrier equilibrium concentration. In this bias interval, in fact, the small bias modulation changes almost exclusively the electron concentration inside one or more QWs. The profile in this bias interval indicates two main concentration peaks. This does

not mean that there are only two QWs because narrowly spaced QWs give rise to overlapping peaks. When the bias varies between -1 and -2 V, a region with apparent charge in smaller concentration appears. This is the bias interval in which QWs are not filled, and the edge of the space charge region (now well defined) crosses the layer immediately next to the MQW system. When the reverse applied bias is $V_b < -2$ V, eventually the depletion region edge crosses the GaN bulk region and the apparent carrier concentration n_{CV} equals the concentration of donors in the bulk. The presence of a region next to the MQW system with lower apparent charge concentration than in the bulk is generally observed even when the concentration of the GaN layers immediately next to the MQW system is equal to the bulk concentration and is due to the upward bending of the conduction band in the MQW region.^{23,24} The width of this “depleted region” can increase if the doping density in the GaN layer next to the MQW system is lower than the bulk doping density.

C. Deep level transient spectroscopy

Information from C - V profiling is important when performing DLTS characterization. Among the most important parameters of DLTS, in fact, are reverse bias level V_b and filling pulse V_{fill} . These determine the region of the junction where the occupation of deep levels is varied,²⁵ and therefore the region from which the emission of carriers is observed. The possibility of tuning the junction region probed by DLTS is particularly useful in experiments involving semiconductor heterostructures.^{15,16,18,19}

DLTS was performed in a set of samples from the same wafer in the temperature interval of 100 – 300 K. This temperature allowed us to exclude phenomena due to charge carrier freeze-out, occurring at the relatively high temperature $T_{fo} \sim 80$ K due to the high activation energy ($E_A - E_V = 0.2$ eV) of Mg acceptor levels.²⁶ The detection of DLTS peaks with temperature close to T_{fo} can be affected by the increase in the series resistance R . As the capacitance C_m measured at frequency f is related to the real capacitance by²⁷

$$C_m = \frac{C}{1 + (2\pi fRC)^2}, \quad (4)$$

capacitance pulses in negative direction and inverted deep level transients occur when the junction is at temperature close to T_{fo} .²⁸ The temperature interval of 300 – 450 K was also investigated, but no deep levels with detectable concentration were found in this region. From the I - V characteristics, the current level throughout the whole temperature and bias interval considered was always lower than 10 pA, corresponding to a current density lower than 1.6×10^{-8} A/cm². This rules out an important source of artifacts in the capacitance measurements

Deep level transient spectra are shown in Fig. 3(a). Each DLTS spectrum evidences the presence of a dominant peak. This peak is labeled C_+ in the spectrum collected with $V_b = -1$ V and $V_{fill} = 0$ V, with positive sign, and C_- in the spectrum collected with $V_b = -3$ V and $V_{fill} = -2$ V, with negative sign. Peaks with positive amplitude in capacitance-DLTS are

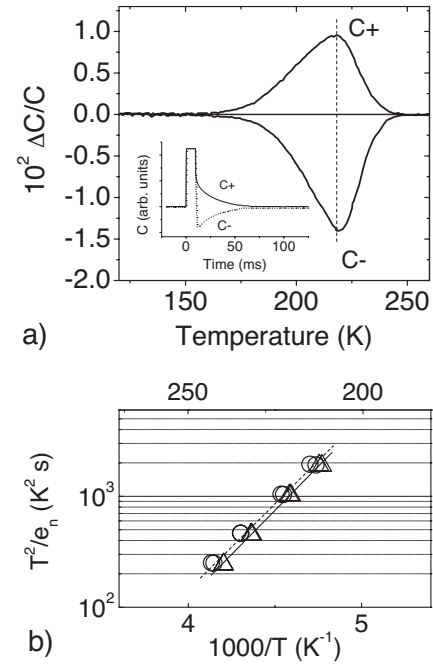


FIG. 3. (a) Positive spectrum: DLTS spectrum collected with $V_b = -1$ V, $V_{fill} = 0$ V, and $t_p = 10$ ms. Negative spectrum: DLTS spectra collected with $V_b = -3$ V, $V_{fill} = -2$ V, and $t_p = 10$ ms. The emission rate is $e_n = 46.5$ s⁻¹. In the inset, capacitance pulses and transients giving rise to peaks C_+ and C_- at $T = 217$ K. (b) The Arrhenius plot shows the overlap of the signatures of C_+ (triangles) and C_- (circles).

usually described as due to the emission of minority carriers, in the present case of holes, from a deep center to the valence band.^{20,25} However, the positive sign of peak C_+ cannot be put in relationship with minority carrier emission. First, the injection of minority carriers should take place by biasing the junction positively, and this does not occur in the present case. Secondly, the Arrhenius analysis [Fig. 3(b)] evidences that C_+ and C_- have the same trap parameters, i.e., an energy $E_C - E_T = 0.25 \pm 0.03$ eV and an apparent capture cross section $\sigma_n \approx 10^{-19}$ cm². Therefore, we infer that C_+ and C_- are related to the same deep level C. This, as a consequence, rules out the possibility that deep level C_+ is related to emission from QW states because this deep level is detected also when portions of the only GaN bulk are probed.

The amplitude of peak C was profiled in the following way: DLTS amplitude was recorded at $T = 217$ K and emission rate $e_n = 46.5$ s⁻¹. The reverse bias V_b was varied while keeping the filling pulse level $V_{fill} = V_b + 1$ V, i.e., maintaining a constant pulse amplitude equal to 1 V and a constant filling pulse width $t_p = 10$ ms. This allowed us to probe a small region of the device excluding the simultaneous solicitation of deep levels in the bulk and in the MQW region while keeping a good signal from the capacitance transient.²⁹ By keeping the pulse amplitude sufficiently low and varying only the reverse bias level, we were thus able to know in which region of the sample the deep level transitions actually occurred. This knowledge was reached through the comparison of the deep level profile with the apparent charge profile from the C - V characterization (Fig. 2).

As far as the pulse varies the occupation of deep levels in the bulk of the n -type region ($|V_b| > 2.5$ V), the DLTS peak is negative. The uniformity of the concentration of free charge in the bulk allowed us to estimate the concentration of deep level C in this region of the junction. Considering the so-called λ effect,³⁰ the concentration of C is calculated as $N_T = (1.0 \pm 0.1) \times 10^{17} \text{ cm}^{-3}$, about one-fourth of the doping concentration in the bulk.

For $V_b > -2.5$ V, the absolute value of the amplitude of peak C_- tends to decrease. At $V_b = -1.75$ V, the transient is inverted and the amplitude of C becomes positive. The amplitude of peak C_+ has a maximum at $V_b = -1.5$ V, then decreases and becomes negative for $V_b > -0.8$ V. Comparison with the n_{CV} profile indicates clearly that this inversion of the peak occurs when the reverse bias V_b crosses the depleted region immediately right of the MQW region, while the filling pulse level V_{fill} probes the MQW region. The inversion of the peak amplitude thus occurs when the filling pulse affects the occupation of deep levels in the MQW region, where piezoelectric fields are present. This strongly suggests that these fields play a key role in the inversion of the transient. The validity of this hypothesis will be discussed in the next section. It is interesting to notice that the inversion of the transient is not accompanied by the inversion of the capacitance pulse [inset of Fig. 3(a)]. This indicates that the inversion of the transient is inherent to the charge redistribution occurring upon deep level discharge, not to other effects influencing the measurement of the capacitance such as those observed during freeze-out or in the presence of a very high series resistance.^{27,28} The reverse bias value for which the transient becomes negative again ($V_b = -0.8$ V) is such that the MQW region is already filled with conduction band electrons.

It is important to point out that the inversion of the transient is not a peculiarity of deep level C. On performing optical-DLTS experiments (DLTS with optical excitation instead of a bias pulse), we found a deep level with clearly different parameters ($E_C - E_T = 0.10$ eV, $\sigma_n = 5 \times 10^{-22} \text{ cm}^2$) significantly showing the same transient inversion in the same interval of reverse bias values V_b . Finally, the same combined analysis of DLTS and C - V characterization was performed on a slightly different nitride-based LED structure with a single QW, without any inversion of the transient. This result is presented in Fig. 4.

D. Nature of deep level C

For the purpose of this analysis, based on the study of the effect of piezoelectric fields on the emission from a deep level, it is essential to exclude the presence and the influence of other electric fields. Thus, we have to exclude that emission from a deep level related to extended defects with a potential barrier associated occurs.^{31,32} When an extended defect becomes charged, an electric field builds up around the defect and superimposes on the piezoelectric field and on the junction field. Point defects tend to segregate along dislocation lines in GaN: in fact, the same deep traps tend to behave as point defects in dislocation-poor material, and as line defects in dislocation-rich material. Care must be taken,

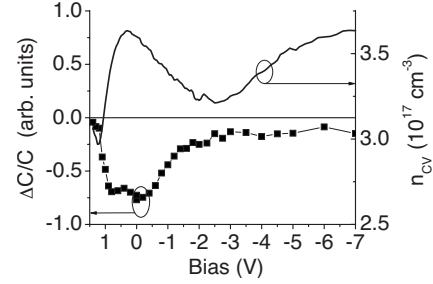


FIG. 4. Apparent carrier profile (solid line, referred to right Y axis) and the peak DLTS signal at $e_n = 46.5 \text{ s}^{-1}$ (squares, referred to left Y axis) at $T = 217$ K in a single-QW LED. The DLTS signal was measured with filling pulse V_{fill} and reverse bias V_b (the latter appearing as abscissa coordinate) related by $V_{fill} = V_b + 1$ V.

therefore, when handling with a material such as n -type epitaxial GaN grown on a mismatched substrate.³³ Several deep levels related to emission from extended defects with potential barrier have been reported in n -type GaN.^{13,34,35} Some of these levels, i.e., E1 (Ref. 34), ED1 (Ref. 13), and A_3 (Ref. 35), have parameters very close to those of deep level C of this work (see Table I) and have been related to extended defects upon analysis of capture kinetics.

The analysis of filling kinetics of deep level C is presented in Fig. 5. The DLTS peak signal was collected at $T = 217$ K and with emission rate $e_n = 46.5 \text{ s}^{-1}$, while the filling pulse width t_p was varied from 10^{-6} to 0.1 s. The filling kinetics for $V_b = -5$ V and $V_{fill} = -4$ V shows a logarithmic behavior for at least four decades (t_p in $10^{-6} - 10^{-2}$ s), while the same measurement for $V_b = -5$ V and $V_{fill} = -2$ V shows a very different behavior, as the amplitude of the DLTS peak remains almost constant throughout the whole interval of pulse widths investigated. The filling behavior with $V_b = -5$ V and $V_{fill} = -3.5$ V is a sort of average between the two aforementioned extrema. This set of observations, in which we carefully chose the DLTS parameters in order to probe only the bulk n -type region, can be explained through the model by Pons.³⁶ According to this model, the filling kinetics is dominated for low filling pulse amplitudes by the Debye tail of free carriers. This translates into a nonexponential dependence of the DLTS amplitude on the filling pulse width, which resembles a logarithmic dependence.³⁶ When the filling pulse amplitude is increased, deep levels are

TABLE I. Deep level parameters in n -type GaN.

Deep level	Energy $E_C - E_T$ (eV)	Cross section σ_n (cm^2)	Concentration n_T (cm^{-3})
C_+ ^a	0.25 ± 0.03	5×10^{-19}	
C_- ^a	0.24 ± 0.03	6×10^{-19}	10^{17}
E1 ^b	0.18–0.27	5.43×10^{-15}	9.5×10^{15}
ED1 ^c	0.23		
A_3 ^d	0.24	3.4×10^{-17}	$10^{13} - 10^{15}$

^aThis work.

^bReference 34.

^cReference 13.

^dReference 35.

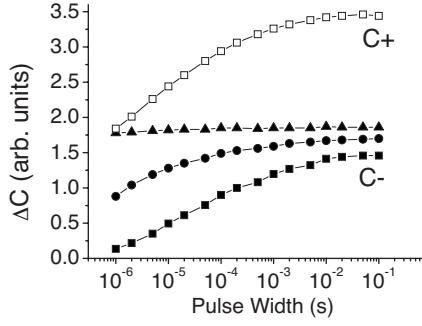


FIG. 5. Amplitude of DLTS signal at $T=217$ K and emission rate $e_n=46.5$ s $^{-1}$ versus filling pulse width. Full symbols refer to the signal giving rise to peak C $_{-}$, measured with the same reverse bias level $V_b=-5$ V and variable filling pulse level; squares, $V_{fill}=-4$ V; circles, $V_{fill}=-3.5$ V; and triangles, $V_{fill}=-2$ V. Empty squares refer to the signal giving rise to peak C $_{+}$, measured with $V_b=-1.5$ V and $V_{fill}=-0.5$ V.

charged by free carriers with the equilibrium bulk concentration, while Debye tails of free carriers play a minor role. This yields an increasingly exponential-like dependence of the DLTS amplitude on the filling pulse width. This trend is reproduced in the case being studied. We are not able to observe the decrease of the DLTS signal for low filling pulses in the case of $V_b=-5$ V and $V_{fill}=-2$ V because the charging up of the deep level is too rapid for detection.

The interpretation of the filling kinetics with $V_b=-1.5$ V and $V_{fill}=-0.5$ V is less straightforward. In this case, the bias parameters of DLTS are such that deep level C has a positive peak with maximum amplitude, and the signal comes mostly from deep levels inside the MQW region. For this reason, it is not meaningful to vary the filling pulse amplitude because this junction region is highly nonuniform. However, one can notice that the dependence of the DLTS signal on the filling pulse width t_p resembles a logarithmic dependence with a constant baseline. The most likely interpretation for this anomalous filling behavior, occurring when the deep level transient is inverted, is the following. First, as the filling pulse charges the quantum well region of the junction with conduction band electrons, carriers in the QWs are in high concentration and tend to fill the deep levels rapidly in their immediate neighborhood, yielding the constant base line. Second, due to the penetration of the wave function of confined electrons in the GaN barriers, deep levels more distant from the QWs tend to fill slowly, yielding the logarithmic part of the filling kinetics.

This set of observations on the filling kinetics of deep level C indicates that this is definitely not related to extended defects giving rise to potential barriers and surrounding fields upon charging-up, but to isolated point defects.

IV. DISCUSSION

A. Transient inversion in presence of piezoelectric fields

The problem of the inversion of deep level transients depending on the bias parameters used in transient spectroscopy experiments is a well-known topic in the case of cur-

rent transients,¹² but no explanation is so far available for the case of capacitance transients. The case of transient inversion in the presence of a heterostructure junction with piezoelectric fields, for instance, has never been considered. In the present case, we deal with a quiescent reverse bias level V_b for which the MQW region of the junction is depleted of conduction band electrons and with a filling pulse level V_{fill} such that the MQW region is filled with conduction band electrons. One of the consequences of this description is the following: during the quiescent reverse bias, it is possible to well define a depletion region width, related to the capacitance C per unit area by

$$C = \frac{\epsilon_s}{w} = \frac{\epsilon_s}{x_n + x_p}, \quad (5)$$

where x_n and $-x_p$ are the limits of the space charge region, provided the junction is located at $x=0$. We assume that the approximation of one-sided junction is valid; therefore, $w \approx x_n$. Applied bias V_b and charge concentration are then related, once solved the Poisson equation, by

$$V_{bi} - V_b = -\frac{1}{\epsilon_s} \int_{-x_p}^{x_n} \rho(x) x dx. \quad (6)$$

The quantity $\rho(x)$ is the space charge density, consisting of different components,

$$\rho(x) = -qN_A(x) + qN_D(x) + q\sigma_{pol}(x) - qn_T(x), \quad (7)$$

where $N_A(x)$ is the net distribution of ionized acceptors on the p side, $N_D(x)$ is the net distribution of ionized donors on the n side (including compensation due to ionized deep traps), $\sigma_{pol}(x)$ is the distribution of polarization charges at each InGaN/GaN interface (considered with its proper sign), and $n_T(x)$ is the distribution of trapped electrons injected in the junction region by a forward bias pulse.

The hypothesis leading to the demonstration of an inverted capacitance transient is the following: the trapped electrons injected during the bias pulse are, as usual, emitted from the deep levels with a characteristic emission rate e_n once the reverse bias is restored at $t=0$. However, differently from the junctions with no piezoelectric field opposed to the junction field, the emitted electrons cannot be collected by the junction, but are trapped in conduction band states in the MQW region. This process can be described through a time-dependent distribution function,

$$-qn_T(x,t) = -qN_T f(x,t), \quad (8)$$

where N_T is the number of trapped electrons per unit area and with the distribution function $f(x,t)$ having the property

$$\int_{-x_p}^{x_n} f(x,t) dx = 1, \quad t \geq 0, \quad (9)$$

stating that no emitted electrons are collected by the junction field. With this property the possibility of positive transients can be demonstrated. For a positive transient to exist, in fact, the following equivalent relationships for capacitance and depletion region width must be verified:

$$C_0 > C_\infty \Leftrightarrow w_0 < w_\infty, \quad (10)$$

where the indices 0 and ∞ refer to the beginning of the transient ($t=0^+$) and infinity, respectively. Thus, at $t=0^+$, one has

$$V_{bi} - V_b = \frac{q}{\epsilon_s} \left\{ - \int_{-x_p}^0 N_A(x) dx + \int_0^{w_0} [N_D(x) + \sigma_{pol}(x) - n_T(x, 0^+)] dx \right\}, \quad (11)$$

while for $t=\infty$,

$$V_{bi} - V_b = \frac{q}{\epsilon_s} \left\{ - \int_{-x_p}^0 N_A(x) dx + \int_0^{w_\infty} [N_D(x) + \sigma_{pol}(x) - n_T(x, \infty)] dx \right\}. \quad (12)$$

Comparing Eqs. (11) and (12) and observing that during the transient the static interface polarization charge σ_{pol} is contained inside the space charge region, one finds

$$\int_0^{w_0} N_D(x) dx - N_T \int_0^{w_0} f(x, 0^+) dx = \int_0^{w_\infty} N_D(x) dx - N_T \int_0^{w_\infty} f(x, \infty) dx. \quad (13)$$

This equation, approximating the donor density as uniform at the depletion region width [$N_D(w_0) \approx N_D(w_\infty)$] and carrying out the integration on the terms including the donor density, yields

$$w_\infty^2 = w_0^2 + \frac{2N_T}{N_D(w_\infty)} \left(\int_0^{w_\infty} f(x, \infty) dx - \int_0^{w_0} f(x, 0^+) dx \right). \quad (14)$$

Thus, the condition for the positive transient is equivalent to a condition on the average value of the distribution of the electrons trapped by deep levels during the bias pulse and emitted during the transient. It is interesting to notice that, by simply omitting the integral at $t=\infty$, Eq. (14) reduces to the standard case in which the emitted charge is collected by the junction and the transient is negative. This also explains the missing transient inversion in the single-QW structure: a single QW system does not have the capability to retrap the emitted carriers in other QWs and to redistribute them spatially. Majority carriers emitted by deep levels are collected by the junction field and transient inversion is not possible in a SQW system.

B. Simulation of charge profiles during deep level transient spectroscopy pulse and reverse bias

The results of Sec. IV A show that a positive transient is possible in a junction if the charge injected by the bias pulse is emitted from the deep levels but not collected by the junc-

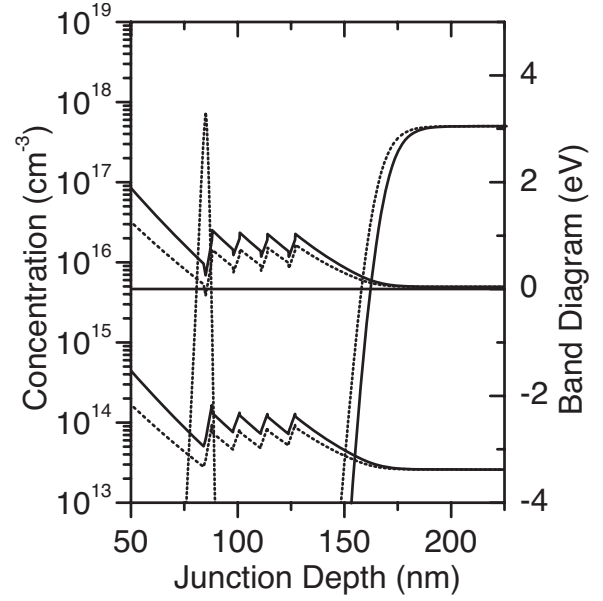


FIG. 6. Simulation of band diagrams and conduction band charge density during reverse bias (solid lines) and filling pulse (dotted lines). The reverse bias and filling pulse levels are $V_b = -1$ V and $V_{fill} = 0$ V, corresponding to the bias region showing deep level transient inversion.

tion. Another condition for the positive sign of the transient is the shift of the distribution of this charge deeper inside the junction. The occurrence of this process is not obvious, thus it will be verified in the following by simulation of conduction band charge distribution during the bias pulse and in the quiescent reverse bias state. Simulation was performed with a one-dimensional Schrödinger-Poisson solver³⁷ on a LED junction structure with typical MQW structural parameters. The MQW structure has inhomogeneous composition: the first QW (closest to the junction) has In fraction $x=0.15$ (as we measured by PC) and a piezoelectric field equal to the measured value $F_{pz}=2.3$ MV/cm; the remaining three QWs have In fraction $x=0.08$ and piezoelectric field $F_{pz}=1.4$ MV/cm.³ Photocurrent and cathodoluminescence experiments performed on the same samples confirm the non-homogeneity of the MQW system.^{38,39} The well width is $t_w=3$ nm and the interwell distance $t_b=10$ nm. The MQW system has a donor concentration $N_D=10^{17}$ cm⁻³. A 100 nm thick GaN spacer layer with donor concentration $N_D=2 \times 10^{17}$ cm⁻³ separates the MQW system from the GaN bulk, doped with $N_D=4 \times 10^{17}$ cm⁻³.

The results of the simulation are shown in Fig. 6. When the bias is at level $V_b=-1$ V (reverse bias, solid lines), the edge of the depletion region is well defined and lies in the less doped spacer layer. This is the bias level for which the n_{CV} profile crosses a region depleted of free charge (Fig. 2). When the bias level is $V_{fill}=0$ V (filling pulse, dashed lines), only the first QW of the MQW system is filled with conduction band electrons, while the distribution of free carriers in the spacer layer shifts only slightly. Thus, mostly traps in the first QW and in its immediate neighborhood are filled. When the reverse bias level is restored, these traps next to the first QW emit the electrons, but there is no way for these elec-

trons to be collected by the junction due to the barrier formed by the whole MQW system, an effect arising from the presence of piezoelectric fields in the MQW system. Moreover, the emitted electrons may be well distributed over the whole MQW system. This process appears less likely for a structure with homogeneous In fraction, where the QWs on the right-hand side of the MQW system would be more difficult to reach because they are lying higher in energy.

C. Comparison between model and experiment

In order to verify the hypothesis for the transient inversion, we estimate here the amplitude of the DLTS inverted peak signal according to the model developed in Sec. IV A [Eq. (14)]. First, from the simulation results the sheet density of electrons injected in the first QW is $n_s = 3 \times 10^{11} \text{ cm}^{-2}$ during the forward bias pulse $V_{fill} = 0 \text{ V}$. The donor density at the edge of the depletion region during the reverse bias $V_b = -1 \text{ V}$ is $N_d = 2 \times 10^{17} \text{ cm}^{-3}$. The depletion region edge, according to the simulation, is located at $w \approx 160 \text{ nm}$. The number of trapped electrons is likely to be comparable with the electron sheet density in the QW $N_T \sim n_s$ and the trapped charge, located at the left edge of the MQW system, rearranges itself during the transient and occupies an average depth at the center of the MQW region. This yields a difference between the average depths of charge distribution [difference between the two integrals in Eq. (14)] equal to about 25 nm. With these values, we find that the relative variations of depth and capacitance before and after the transient are $\Delta w/w = \Delta C/C = 0.015$. This value is well in agreement with the experimental value measured at the DLTS peak (Fig. 3). The density of electrons per unit area equal to $N_T = 3 \times 10^{11} \text{ cm}^{-2}$ corresponds to a deep level concentration $n_T = 5 \times 10^{17} \text{ cm}^{-3}$ if we suppose that the deep levels charging up are concentrated in a region of width about double as that of the QW. This deep level density is roughly equal to the density of shallow donors in the bulk GaN, and five times as high as the deep level density measured in the bulk material. This discrepancy could be explained in two ways. First, the value found for n_T in the QW region is overestimated and could be reduced by admitting that electrons are trapped in a more extended region. Second, the density of deep levels

increases in the MQW region with respect to the bulk density due to the presence of interfaces and electric fields, which could yield defect segregation. In any case, the concentration of deep levels in the MQW region is not lower than that in the bulk and can give rise to important effects, such as compensation or strong influence on the concentration of electrons.¹⁴ It is worth noting that the high concentration of the deep level is not required for transient inversion, as this is exclusively due to the presence of piezoelectric fields.

V. CONCLUSIONS

DLTS characterization of InGaN/GaN MQW light-emitting diodes has been carried out. Depending on the bias parameters, an anomalous inversion of the capacitance transient of the dominant deep level C was observed. Deep level C is a majority carrier trap, related to isolated point defects. The inversion of its capacitance transient occurs when the reverse bias leaves the MQW region depleted and when the filling pulse injects carriers in the MQW region, as the analysis of the C - V profiles indicates. Piezoelectric fields, measured by means of photocurrent, are intense enough for the formation of an average positive field opposite to the negative junction field in the MQW layer. This prevents majority carriers emitted by the traps from being collected by the junction, maintaining them in conduction band states in the MQW region. When the redistribution of electrons during the transient shifts their center of mass deeper toward the bulk, the capacitance transient is positive. The validity of this hypothesis was tested by simulating the MQW structure, yielding results in substantial agreement with the experimental data.

ACKNOWLEDGMENTS

The authors would like to acknowledge OSRAM Opto Semiconductors for providing the samples. This work was partially supported by the Italian MIUR under the PRIN project “High brightness, high efficiency GaN Light Emitting Diodes for future solid-state lighting systems” (2005–2007), coordinated by E. Zanoni. The authors would also like to acknowledge M. Meneghini, M. Pavesi, and F. Rossi for fruitful discussion.

*Corresponding author; Tel.: +39-051-2095806; lorenzo.rigutti@unibo.it

¹F. Bernardini, V. Fiorentini, and D. Vanderbilt, Phys. Rev. B **56**, R10024 (1997).

²T. Takeuchi, C. Wetzel, S. Yamaguchi, H. Sakai, H. Amano, I. Akasaki, Y. Kaneko, S. Nagakawa, Y. Yamaoka, and N. Yamada, Appl. Phys. Lett. **73**, 1691 (1998).

³V. Fiorentini, F. Bernardini, and O. Ambacher, Appl. Phys. Lett. **80**, 1204 (2002).

⁴I. H. Brown, I. A. Pope, P. M. Smowton, P. Blood, D. J. Thomson, W. W. Chow, D. P. Bour, and M. Kneissl, Appl. Phys. Lett. **86**, 131108 (2005).

⁵Y. D. Jho, J. S. Yahng, E. Oh, and D. S. Kim, Appl. Phys. Lett. **79**, 1130 (2001).

⁶F. Renner, P. Kiesel, G. H. Döhler, M. Kneissl, C. G. Van de Walle, and N. M. Johnson, Appl. Phys. Lett. **81**, 490 (2002).

⁷G. Franssen, P. Perlin, and T. Suski, Phys. Rev. B **69**, 045310 (2004).

⁸M. Leroux, N. Grandjean, M. Laugt, J. Massies, B. Gil, P. Lefebvre, and P. Bigenwald, Phys. Rev. B **58**, R13371 (1998).

⁹J. M. Shah, Y. L. Li, T. Gessmann, and E. F. Schubert, J. Appl. Phys. **94**, 2627 (2003).

¹⁰M. Zervos, A. Kostopoulos, G. Constantinidis, M. Kambayaki, and A. Georgakilas, J. Appl. Phys. **91**, 4387 (2002).

- ¹¹R. J. Kaplar, S. Kurtz, and D. Koleske, Proceedings of the Materials Research Society Fall 2005 Meeting (unpublished), Paper No. 0892-FF32-01.
- ¹²A. Cavallini, G. Verzellesi, A. F. Basile, C. Canali, A. Castaldini, and E. Zanoni, *J. Appl. Phys.* **94**, 5297 (2003).
- ¹³O. Yastrubchak, T. Wosinski, A. Makosa, T. Figielski, S. Porowski, I. Grzegory, R. Czernecki, and P. Perlin, *Eur. Phys. J.: Appl. Phys.* **27**, 201 (2004).
- ¹⁴F. Capotondi, G. Biasiol, I. Vobornik, L. Sorba, F. Giazotto, A. Cavallini, and B. Fraboni, *J. Vac. Sci. Technol. B* **22**, 702 (2004).
- ¹⁵N. Debbar, D. Biswas, and P. Bhattacharya, *Phys. Rev. B* **40**, 1058 (1989).
- ¹⁶Q. Wang, F. Lu, D. Gong, X. Chen, J. Wang, H. Sun, and X. Wang, *Phys. Rev. B* **50**, 18226 (1994).
- ¹⁷Q. S. Zhu, X. B. Wang, Z. T. Zhong, X. C. Zhou, Y. P. He, Z. P. Cao, G. Z. Zhang, J. Xiao, X. H. Sun, H. Z. Yang, and Q. G. Du, *Phys. Rev. B* **57**, 12388 (1998).
- ¹⁸K. Schmalz, I. N. Yassievich, H. Rücker, H. G. Grimmeiss, H. Frankenfeld, W. Mehr, H. J. Osten, P. Schley, and H. P. Zeindl, *Phys. Rev. B* **50**, 14287 (1994).
- ¹⁹K. Schmalz, I. N. Yassievich, E. J. Collart, and D. J. Gravesteijn, *Phys. Rev. B* **54**, 16799 (1996).
- ²⁰J. W. Kim, G. H. Song, and J. W. Lee, *Appl. Phys. Lett.* **88**, 182103 (2006).
- ²¹P. Blood and J. W. Orton, *The Electrical Characterization of Semiconductors: Majority Carriers and Electron States* (Academic, London, 1990).
- ²²J. Wu, W. Walukiewicz, K. M. Yu, J. W. Ager III, E. E. Haller, H. Lu, and W. J. Schaff, *Appl. Phys. Lett.* **80**, 4741 (2002).
- ²³B. M. Tschirner, F. Morier-Genoud, D. Martin, and F. K. Reinhart, *J. Appl. Phys.* **79**, 7005 (1996).
- ²⁴C. R. Moon, B. D. Choe, S. D. Kwon, H. K. Shin, and H. J. Lim, *J. Appl. Phys.* **84**, 2673 (1998).
- ²⁵G. L. Miller, D. V. Lang, and L. C. Kimerling, *Annu. Rev. Mater. Sci.* **7**, 377 (1977).
- ²⁶S. Strite and H. Morkoç, *J. Vac. Sci. Technol. B* **10**, 1237 (1992).
- ²⁷D. K. Schroder, *Semiconductor Material and Device Characterization* (Wiley-Interscience, New York, 1998).
- ²⁸F. Rossi, M. Pavesi, M. Meneghini, G. Salviati, M. Manfredi, G. Meneghesso, A. Castaldini, A. Cavallini, L. Rigutti, U. Strauss, U. Zehnder, and E. Zanoni, *J. Appl. Phys.* **99**, 053104 (2006).
- ²⁹This could be, in principle, a procedure for the profiling of the deep level concentration equivalent to the so-called double-DLTS (DDLTS), which is regarded as more accurate in homogeneous junctions [see, for instance, P. Blood and J. W. Orton, *The Electrical Characterization of Semiconductors: Majority Carriers and Electron States* (Academic, London, 1990)]. However, concentration profiling was a minor issue in the present case, and DDLTS was not considered a viable investigation technique because it varies the occupation of deep levels in a wide portion of the junction.
- ³⁰D. C. Look and J. R. Sizelove, *J. Appl. Phys.* **78**, 2848 (1995).
- ³¹T. Figielski, *Phys. Status Solidi* **6**, 429 (1964).
- ³²W. Schröter, J. Kronewitz, U. Gnauert, F. Riedel, and M. Seibt, *Phys. Rev. B* **52**, 13726 (1995).
- ³³Z.-Q. Fang, D. C. Look, and L. Polenta, *J. Phys.: Condens. Matter* **14**, 13061 (2002).
- ³⁴H. K. Cho, C. S. Kim, and C.-H. Hong, *J. Appl. Phys.* **94**, 1485 (2003).
- ³⁵C. B. Soh, S. J. Chua, H. F. Lim, D. Z. Chi, W. Liu, and S. Tripathy, *J. Phys.: Condens. Matter* **16**, 6305 (2004).
- ³⁶D. Pons, *J. Appl. Phys.* **55**, 3644 (1983).
- ³⁷M. Grundmann, BANDENG (<http://my.ece.ucsb.edu/mgrundmann/bandeng.htm>).
- ³⁸L. Rigutti, A. Castaldini, M. Meneghini, and A. Cavallini, *Semicond. Sci. Technol.* **23**, 025004 (2008).
- ³⁹F. Rossi, M. Pavesi, M. Meneghini, G. Salviati, M. Manfredi, and E. Zanoni (unpublished).